

Semi-supervised Embedding Learning for High-dimensional Bayesian Optimization

Jingfan Chen

JINGFAN.CHEN@SMAIL.NJU.EDU.CN

Guanghui Zhu*

GUANGHUI.ZHU@SMAIL.NJU.EDU.CN

Rong Gu

GURONG@NJU.EDU.CN

Chunfeng Yuan

CFYUAN@NJU.EDU.CN

Yihua Huang*

YHUANG@NJU.EDU.CN

State Key Laboratory for Novel Software Technology

Nanjing University

Nanjing 210023, China

Editor:

Abstract

Bayesian optimization is a broadly applied methodology to optimize the expensive black-box function. Despite its success, it still faces the challenge from the high-dimensional search space. To alleviate this problem, we propose a novel Bayesian optimization framework, which finds a low-dimensional space to perform Bayesian optimization through a semi-supervised, iterative, and embedding learning-based method (SILBO). SILBO incorporates both labeled and unlabeled points acquired from the acquisition function of Bayesian optimization to guide the learning of embedding space. To accelerate the learning procedure, we present a randomized method for generating the projection matrix. Furthermore, to map from the low-dimensional space to the high-dimensional original space, we propose two mapping strategies: SILBO-BU and SILBO-TD according to the evaluation overhead of the objective function. Experimental results on both synthetic function and hyperparameter optimization tasks demonstrate that SILBO outperforms the existing state-of-the-art high-dimensional Bayesian optimization methods.

Keywords: Bayesian Optimization, High-dimensional Optimization, Semi-supervised Learning, Dimension Reduction, Embedding Learning,

1. Introduction

As a well-established approach for sample-efficient global optimization of black-box functions that are expensive to evaluate, Bayesian optimization (BO) is used in many tasks such as hyperparameter tuning (Hutter et al., 2011; Bergstra et al., 2011; Snoek et al., 2012), neural architecture search (Kandasamy et al., 2018), and chemical structure search (Gmez-Bombarelli et al., 2018). BO provides a principled method for finding the global optimum of black-box function: using the cheap probability surrogate model of black-box function as the input to the acquisition function, repeatedly considering the trade-off between exploitation and exploration to select the promising points. The surrogate model is constructed

*. Corresponding authors with equal contribution

based on the evaluation values observed so far. A widely-used surrogate model is Gaussian Process regression, which provides the uncertainty quantification of the function value by imposing a Gaussian Process prior.

While BO provides such an automated procedure, it still faces a huge challenge in high-dimensional scenarios. To ensure the converge for learning the function response value, the sample complexity depends exponentially on the number of dimensions (Shahriari et al., 2016). In practice, BO is limited to the optimization problem with around 20 dimensions when using Gaussian Process regression as a surrogate model (Frazier, 2018).

To handle high-dimensional Bayesian optimization, many methods have been proposed. Based on the assumption that only a small number of dimensions influence the response value of the objective function, the embedding methods perform BO on a low-dimensional space. The corresponding projection matrix can be constructed randomly (Wang et al., 2013; Nayebi et al., 2019), or learned actively (Djolonga et al., 2013; Zhang et al., 2019). Some methods impose an additive structure on the objective function (Gardner et al., 2017; Kandasamy et al., 2015). Besides, many methods start from the way of learning low-dimensional embedding and find an effective subspace through nonlinear dimension reduction (Lu et al., 2018). However, there are two limitations in the existing methods. First, the projection matrix is immutable. Once the generated low-dimensional embedding cannot represent the intrinsic structure of the objective function, finding the global optimum through Bayesian optimization will become very difficult. Second, the low-dimensional space is learned in a supervised way. The label of each point indicates the response value of the black-box function. To learn an effective low-dimensional space, a large number of labeled points are required, which leads to huge computation costs especially when the evaluation overhead of the objective function is expensive.

In this paper, we propose a novel framework called SILBO¹ to mitigate the problem of *the curse of dimensionality* by learning the effective low-dimensional space iteratively through the semi-supervised dimension reduction method. After a low-dimensional space is identified, Bayesian optimization is performed in the low-dimensional space, leading to a stable and reliable estimation of the global optimum. Specifically, the contribution of this paper is as follows:

- We propose an iterative method in SILBO to update the projection matrix dynamically. During each iteration of BO, a semi-supervised low-dimensional embedding learning method is proposed to construct the projection matrix by utilizing both labeled and unlabeled points acquired from the acquisition function of BO.
- To accelerate the semi-supervised dimension reduction, we further propose a randomized method to compute the high-dimensional generalized eigenvalue problem efficiently. We also analyze its time complexity in detail.
- Furthermore, to map from the low-dimensional space to the high-dimensional original space, we propose two mapping strategies: SILBO-TD and SILBO-BU according to the evaluation overhead of the objective function.

1. SILBO stands for **S**emi-supervised, **I**terative, and **L**earning-based **B**ayesian **O**ptimization. The code is available at <https://github.com/cjfcsjt/SILBO>.

- Experimental results on both synthetic function and neural network hyperparameter optimization tasks reveal that SILBO outperforms the existing state-of-the-art high-dimensional Bayesian optimization methods.

The rest of this paper is organized as follows. Section 2 gives an overview of related work. Section 3 states the problem and lists relevant background materials. The SILBO algorithm is proposed in Section 4. The experimental evaluation is presented in Section 5 and the conclusion is given in Section 6.

2. Related Work

Bayesian optimization has achieved great success in many applications with low dimensions (Kandasamy et al., 2017; Klein et al., 2017; Swersky et al., 2013; Wu et al., 2019, 2017; Hernández-Lobato et al., 2016). However, extending BO to high dimensions is still a challenge. Recently, the high-dimensional BO has received increasing attention and a large body of literature has been devoted to addressing this issue.

Given the assumption that only a few dimensions play a decisive role, the linear low-dimensional embedding method achieves dimension reduction using a projection matrix. In REMBO (Wang et al., 2013), the projection matrix is randomly generated according to Gaussian distribution. The promising points are searched in the low-dimensional space by performing Gaussian Process regression and then mapped back to the high-dimensional space for evaluation. It has been proven that REMBO has a great probability to find the global optimum by convex projection, although the high probability is not guaranteed when the box bound exists. Another problem of REMBO is the over-exploration of the boundary. To address the over exploration, a carefully-selected bound in the low-dimensional embedding space was proposed (Binois et al., 2019), which finds the corresponding points in the high-dimensional space by solving a quadratic programming problem. The BOCK algorithm (Oh et al., 2018) scales to the high-dimensional space using a cylindrical transformation of the search space. HeSBO (Nayebi et al., 2019) employs the count sketch method to alleviate the over-exploration of the boundary and use the hash technique to improve computational efficiency. HeSBO also shows that the mean and variance function of Gaussian Process do not deviate greatly under certain condition. However, the above-mentioned methods only use the prior information to generate the projection matrix randomly and do not employ the information of the actual initial points to learn a low-dimensional embedding actively.

Different from the previous methods, the learning-based methods have been proposed. SIRBO (Zhang et al., 2019) uses the supervised dimension reduction method to learn a low-dimensional embedding, while SI-BO (Djolonga et al., 2013) employs the low-rank matrix recovery to learn the embedding. However, the low-dimensional embedding learned by these methods is immutable. Once the projection matrix is generated according to the initial points, it will not be updated. In some scenarios, because of the small number of initial points that have been evaluated, the low-dimensional embedding space cannot accurately reflect the information of the objective function.

Another way for handling the high-dimensional BO is to assume an additive structure (Gardner et al., 2017) of the objective function. Typically, ADD-BO (Kandasamy et al., 2015) optimizes the objective function on a disjoint subspace decomposed from the high-dimensional space. Unfortunately, the additive assumption does not hold in most practical

applications. Besides, the non-linear embedding method is also attractive (Eissman et al., 2018; Lu et al., 2018; Moriconi et al., 2019). These non-linear methods use the Variational Autoencoder (VAE) to learn a low-dimensional embedding space. The advantage of non-linear learning methods is that points in the original space can be easily reconstructed through the non-linear mapping. However, training VAE requires a large number of points. When the evaluation cost of the objective function is expensive, the non-linear embedding method is almost impractical.

In this paper, we focus on the linear low-dimensional embedding method and propose an iterative, semi-supervised method to learn the embedding.

3. Preliminary

In this section, we give the problem setup and introduce Bayesian optimization (BO), semi-supervised discriminant analysis (SDA), and slice inverse regression (SIR).

3.1 Problem Setup

Consider the black-box function $f : \mathcal{D} \rightarrow [0, 1]$, defined on a high-dimensional d and continuous domain $\mathcal{D} = [-1, 1]^d \subset \mathbb{R}^d$. $f(\mathbf{x})$ is computationally expensive and may be non-convex. Given $\mathbf{x} \in \mathcal{D}$, we can only access the noisy response value y extracted from $f(\mathbf{x})$ with noise $\epsilon \sim \mathcal{N}(0, \sigma^2)$. Also, we assume that the objective function contains $r \leq d$ intrinsic dimensions. In other words, given an embedding matrix $B \in \mathbb{R}^{r \times d}$ with orthogonal rows and a function $g : \mathbb{R}^r \rightarrow [0, 1]$, $f(\mathbf{x}) = g(B\mathbf{x})$. Our goal is to find the global optimum.

$$\mathbf{x}^* = \arg \max_{\mathbf{x} \in \mathcal{D}} f(\mathbf{x}) \quad (1)$$

3.2 Bayesian Optimization

Bayesian optimization is an iterative framework, which combines a surrogate model of the black-box function with a search strategy that tries to find possible points with large response values. Given t observation points $\mathbf{x}_1, \dots, \mathbf{x}_t \in \mathcal{D}$ and their corresponding evaluation values y_1, \dots, y_t , the surrogate model is usually Gaussian Process regression that imposes a prior, $f(\mathbf{x}_{1:t}) \sim \mathcal{GP}(\mu(\mathbf{x}_{1:t}), k(\mathbf{x}_{1:t}, \mathbf{x}_{1:t}))$, to the objective function with mean function μ at each \mathbf{x}_i and covariance function or kernel k at each pair of points $(\mathbf{x}_i, \mathbf{x}_j)$. The kernel function describes the similarity between inputs. One of the widely-used kernel functions is the Matrn kernel. Then, given a new point \mathbf{x}^* , the prediction of the response value can be calibrated by the posterior probability distribution (noise-free).

$$f(\mathbf{x}^*) | f(\mathbf{x}_{1:t}) \sim \mathcal{N}(\mu_t(\mathbf{x}^*), \sigma_t(\mathbf{x}^*)) \quad (2)$$

$$\mu_t(\mathbf{x}^*) = k(\mathbf{x}^*, \mathbf{x}_{1:t}) k(\mathbf{x}_{1:t}, \mathbf{x}_{1:t})^{-1} (f(\mathbf{x}_{1:t}) - \mu(\mathbf{x}_{1:t})) + \mu(\mathbf{x}^*) \quad (3)$$

$$\sigma_t(\mathbf{x}^*) = k(\mathbf{x}^*, \mathbf{x}^*) - k(\mathbf{x}^*, \mathbf{x}_{1:t}) k(\mathbf{x}_{1:t}, \mathbf{x}_{1:t})^{-1} k(\mathbf{x}_{1:t}, \mathbf{x}^*) \quad (4)$$

At each iteration of Bayesian optimization, the predictive mean and variance are regarded as uncertainty quantification, supporting the subsequent acquisition function optimization. The acquisition function tries to balance between exploration (high variance)

and exploitation (high mean value). The commonly-used acquisition function for searching promising points is UCB (Upper Confidence Bound) (Srinivas et al., 2010). UCB tries to select the next point with the largest plausible response value according to Equation 5.

$$\mathbf{x}_{t+1} = \arg \max_{\mathbf{x} \in \mathcal{D}} \mu_t(\mathbf{x}) + \beta_t^{1/2} \sigma_t(\mathbf{x}) \quad (5)$$

where β_t is a parameter set used to achieve the trade-off between exploration and exploitation. In this work, we also experiment with EI (Expected Improvement) (Snoek et al., 2012), which is another popular acquisition function.

3.3 Semi-supervised Discriminant Analysis

Semi-supervised discriminant analysis (SDA) (Cai et al., 2007) is a semi-supervised linear dimension reduction algorithm that leverages both labeled and unlabeled points. SDA aims to find a projection that reflects the discriminant structure inferred from the labeled data points, as well as the intrinsic geometrical structure inferred from both labeled and unlabeled points. SDA is an extension of linear discriminant analysis (LDA). The original LDA aims to find a projection β such that the ratio of the between-class scatter matrix S_b to the total within-class scatter matrix S_t is maximized. When the number of training data is small, it can easily lead to overfitting. SDA solves this problem by introducing a regularizer $J(\beta)$ combined with unlabeled information.

$$\beta^* = \arg \max_{\beta} \frac{\beta^\top S_b \beta}{\beta^\top S_t \beta + \alpha J(\beta)} \quad (6)$$

where α is a coefficient used to balance between model complexity and experience loss.

$J(\beta)$ is constructed by considering a graph S incorporating neighbor information of the labeled points and the unlabeled points, where S_{ij} indicates whether x_i and x_j are neighbors. Motivated from spectral dimension reduction (Belkin and Niyogi, 2001), the regularizer can be defined as $J(\beta) = \sum_{ij} (\beta^\top x_i - \beta^\top x_j)^2 S_{ij}$ for any two points x_i and x_j . Then, given the dataset X , $J(\beta)$ can be written as:

$$J(\beta) = 2\beta^\top X(D - S)X^\top \beta = 2\beta^\top X L X^\top \beta \quad (7)$$

where D is a diagonal matrix, $D_{ii} = \sum_j S_{ij}$, and L is a Laplacian matrix (Chung, 1997). Finally, SDA can be reformulated as solving the following generalized eigenvalue problem.

$$S_b \beta = \lambda(S_t + \alpha X L X^\top) \beta \quad (8)$$

3.4 Slice Inverse Regression

Sliced inverse regression (SIR) (Li, 1991) is a supervised dimension reduction method for continuous response values. SIR aims to find an effective low-dimensional space. The dimension reduction model is:

$$Y = g(\beta_1^\top \mathbf{x}, \dots, \beta_r^\top \mathbf{x}, \epsilon) \quad (9)$$

Here, Y is the response variable, $\mathbf{x} \in \mathbb{R}^d$ is an input vector, g is an unknown function with $r + 1$ arguments. $\{\beta_1, \dots, \beta_r\}$ denotes orthogonal projection vectors, r denotes the

dimensions of the *e.d.r.* (effective dimension reducing) space and ϵ is noise. The core idea of SIR is to swap the positions of \mathbf{x} and Y . The algorithm cuts response value Y into H slices and consider the H -dimensional inverse regression curve $E(\mathbf{x}|Y) = (E(\mathbf{x}_1|Y), \dots, E(\mathbf{x}_H|Y))$ rather than regressing Y on \mathbf{x} directly. SIR assumes the existence of *e.d.r.* directions, and the curve that just falls into an r -dimensional space. SIR finds the *e.d.r.* directions by minimizing the total within-slice scatter Σ_x and maximize the between-slice scatter Σ_η . Similar to LDA, the problem can be reformulated as solving the following generalized eigenvalue problem.

$$\Sigma_\eta \beta = \lambda \Sigma_x \beta \quad (10)$$

4. The SILBO Algorithm

In this section, we propose a framework that addresses the high-dimensional optimization challenge by learning a low-dimensional embedding space \mathcal{Z} associated with a projection matrix B . To learn the intrinsic structure of the objective function effectively, we iteratively update B through semi-supervised dimension reduction. Moreover, we propose a randomized method to accelerate the computation of the embedding matrix B in the high-dimensional scenario. By performing BO on the learned low-dimensional space \mathcal{Z} , the algorithm can approach the $\mathbf{z}^* \in \mathcal{Z}$ that corresponds to the optimum $\mathbf{x}^* \in \mathcal{D}$ as close as possible.

Given the labeled points X_l and unlabeled points X_u where the label represents the evaluation value of the corresponding point, SILBO consists of three tightly-connected phases:

- embedding learning, which tries to find an effective low-dimensional space \mathcal{Z} of the objective function by utilizing both X_l and X_u ;
- performing Gaussian Process regression on the learned low-dimensional embedding space and selecting candidate points according to the acquisition function of BO;
- evaluating points by the objective function f , then updating the Gaussian Process surrogate model and the projection matrix B .

Algorithm 1 summarizes the three steps. The first step is to construct the projection matrix B and find an effective low-dimensional space that can keep the information of the original space as much as possible, where X_u is the unlabeled points obtained by acquisition function and X_l is the labeled points that have been evaluated.

The second step is to find the possible low-dimensional optimum $\mathbf{z}_l \in \mathcal{Z}$ which maximizes the acquisition function α and select several promising unlabeled points $\mathbf{z}_u \in \mathcal{Z}$ that can be used to update B in the next iteration. Then, \mathbf{z}_l and \mathbf{z}_u are mapped back to the high-dimensional space \mathcal{D} through a specific mapping $h: \mathcal{Z} \rightarrow \mathcal{D}$ to get \mathbf{x}_l and \mathbf{x}_u .

Finally, we compute y by evaluating the objective function f on x_l and update the GP model by (z_l, y) . The x_l and x_u will be added to X_l and X_u respectively for updating the embedding in the next iteration.

The low-dimensional embedding is learned through SIR combined with the semi-supervised technique. The between-slice scatter matrix Σ_η and total within-slice scatter matrix Σ_x are constructed by utilizing the local information as well as the unlabeled points. Then, B

is obtained through solving the generalized eigenvalue problem. Based on the randomized SVD method, Algorithm 2 is proposed to speed up the solution to this problem. Moreover, we carefully analyze the mapping h between the low-dimensional space and the high-dimensional space and further propose two strategies for the scenarios with different evaluation costs.

Algorithm 1: SILBO

Input: Objective function f , acquisition function α , high dimension d , effective dimension r

Output: The optimum x^*

- 1 Initialize samples X_u^0, X_l^0 with size n_u and n_l ;
- 2 Construct B_0 with Algorithm 2;
- 3 Let $D_0 = \{B_0 X_l^0, f(X_l^0)\}$;
- 4 Construct Gaussian Process regression model based on D_0 ;
- 5 $Z_l^0 = \emptyset, Y_0 = \emptyset$;
- 6 **for** $t = 1$ to N **do**
- 7 $Z_u^t = \emptyset$;
- 8 Generate random point set C from the low-dimensional space;
- 9 $z_l = \arg \max_{z \in C} \alpha(z)$;
- 10 $Z_l^t = Z_l^{t-1} \cup z_l$;
- 11 $C = C - z_l$;
- 12 **for** $n = 1$ to n_u **do**
- 13 $z_u = \arg \max_{z \in C} \alpha(z)$;
- 14 $Z_u^t \cup z_u$;
- 15 $C = C - z_u$;
- 16 **end**
- 17 Construct X_l^t, X_u^t, D_t based on Z_l^t, Z_u^t ;
- 18 Update Gaussian process regression model based on D_t ;
- 19 Update B_t with Algorithm 2 based on X_u^t, X_l^t and Y_t ;
- 20 **end**

4.1 Semi-supervised Embedding Learning

The assumption is that there is a low-dimensional space that preserves the information of the objective function $f(\mathbf{x})$ defined in the high-dimensional space. In other words, the dimensionality of \mathcal{D} can be reduced without losing the essential information to predict response values Y . Meanwhile, if there are enough evaluated points for the initialization of Bayesian optimization, we may be able to explore the intrinsic structure of $f(\mathbf{x})$ through these points. However, for optimization problems with high computational cost, only a few evaluated points are available. Thus, it is difficult to learn proper embedding only through them. In such a case, reasonable and effective use of unevaluated points acquired from the acquisition function of BO will be helpful for embedding learning.

Although SDA provides an effective strategy to incorporate the unlabeled data, it is only suitable for classification problems. Therefore, we need to extend it to the scenarios

where the response value is continuous. At the same time, SIR is suitable for the supervised dimension reduction tasks in the continuous domain. SIR aims to find the e.d.r directions to minimize the total within-slice scatter and maximize the between-slice scatter, the purpose of which is very similar to that of LDA. In fact, SIR is equivalent to LDA (Wu et al., 2010). Due to the equivalence of these two methods, along with the fact that SDA is an extension of LDA, we can employ such discreteness brought by the slicing technique in SIR to apply SDA to the continuous domain. Next, we introduce how to construct semi-SIR to learn a low-dimensional subspace embedding.

We first assume that nearby points often have not only close response values but also similar low-dimensional representations. Furthermore, we sort the evaluated points according to their response values and cut them into H slices. This process can be equivalent to that the labeled points belong to H different classes. Therefore, similar to SDA (Cai et al., 2007), our problem can be reformulated as follows. Given labeled points $X_l \in \mathbb{R}^{n_l \times d}$ and unlabeled points $X_u \in \mathbb{R}^{n_u \times d}$, n_l and n_u denote the number of the labeled and unlabeled points respectively, we aim to find the embedding matrix B through solving:

$$X^\top W X \beta = \lambda X^\top (\hat{I} + \alpha L) X \beta \quad (11)$$

where $X \in \mathbb{R}^{n \times d}$ denotes a centered data matrix whose rows represent n samples in \mathbb{R}^d , $n = n_u + n_l$. W is a $n \times n$ weight matrix. \hat{I} can be expressed as:

$$\hat{I} = \begin{bmatrix} I & 0 \\ 0 & 0 \end{bmatrix} \quad (12)$$

where I is a $n_l \times n_l$ identity matrix.

Note that the between-slice scatter matrix $X^\top W X$ can be written in an elegant linear algebraic formulation.

$$X^\top W X = X^\top \Omega \Omega^\top X = X^\top \begin{bmatrix} \Omega_l \Omega_l^\top & 0 \\ 0 & 0 \end{bmatrix} X \quad (13)$$

where $\Omega_l \in \mathbb{R}^{n_l \times H}$ denotes the rescaled slice membership matrix for those evaluated samples with $\Omega_{l_{ij}} = 1/\sqrt{n_j}$ if the i -th sample of X_l is a member of the j -th slice. Otherwise, $\Omega_{l_{ij}} = 0$. n_j denotes the number of the samples in the j -th slice.

For the labeled points in the same slice, their response values are very close, but this closeness may not be retained in \mathcal{D} . There could be a small number of points that are far away from others in each slice. Although these *outliers* may indicate that there exist other areas with large response values of the objective function, they are likely to interfere with the embedding we have learned. Thus, to reveal the main information of the objective function as much as possible, we employ the localization technique. By strengthening the local information of each slice, the degeneracy issue in the original SIR can be mitigated (Wu et al., 2010). Next, we illustrate how to construct W in Equation 13 with the local information.

We note that Ω_l in Equation 13 is a block matrix, and each block corresponds to a slice.

$$\Omega_l = \begin{pmatrix} \Omega_l^1 & & \\ & \ddots & \\ & & \Omega_l^H \end{pmatrix} \quad (14)$$

For the original between-slice scatter $X^\top WX$, Ω_l can only indicate whether a sample point belongs to a slice. Here, we will strengthen the localization information by introducing a localized weight. For those evaluated samples, we let $\Omega_{ij}^h = 1/k_h$ if the i -th sample belongs to the k -nearest neighbors of the j -th sample (j can equal to i) in the h -th slice. Otherwise, $\Omega_{ij}^h = 0$. H denotes the number of slices, k is a parameter for k NN, and k_h is the number of neighbor pairs in the h -th slice.

On the other hand, if these *outliers* contain enough information, then through the iterative process of Bayesian optimization, we have a great probability to get other points near *outliers*. As a result, the number of these *outliers* may expand and become the leading samples in their slice to guide the generation of embedding. Therefore, it is necessary to update the projection matrix B iteratively.

In summary, we aim to estimate the intrinsic structure of the objective function and find an effective subspace that reflects the large response value. Then, we are in a better position to identify the possible global optimum. Therefore, in combination with Bayesian optimization whose acquisition function will provide us candidate points with potentially large response values, semi-supervised dimension reduction can alleviate overfitting caused by the small size of labeled points. Thus, by utilizing both the labeled and unlabeled points, we can learn an r -dimensional space that preserves the intrinsic structure of the objective function better.

4.2 Randomized Semi-supervised Dimension reduction

In the high-dimensional scenario, learning a low-dimensional embedding space still requires a lot of time. The main bottleneck lies in the solution of generalized eigenvalue problem in Equation 11 and the computation of the neighbor information in each slice. The major computation cost of the traditional method such as the two-stage SVD algorithm is the decomposition of the large-scale matrix. Fortunately, the randomized SVD (R-SVD) technique (Halko et al., 2011) shed a light on this problem.

The contribution of R-SVD here is that when the effective dimension $r \ll n < d$, using randomized SVD to approximate a $n \times d$ matrix only requires $O(ndr)$, rather than $O(n^2d)$. Moreover, the empirical results find that when solving the generalized eigenvalue problem, the performance of the randomized algorithm is superior to that of the traditional deterministic method in the high-dimensional case (Georgiev and Mukherjee, 2012). Thus, we first replace the two-stage SVD with R-SVD to accelerate the solution of Equation 11.

We note that the decomposition overhead of the $X^\top \Omega \in \mathbb{R}^{d \times n}$ in Equation 11 is huge when d is large. Thus, we decompose $X^\top \Omega = U_1 S_1 V_1^\top$ using the R-SVD algorithm. Then, the between-slice scatter matrix can be expressed as:

$$X^\top \Omega \Omega^\top X = U_1 S_1^2 U_1^\top \quad (15)$$

Similarly, due to the symmetry of matrix $\hat{I} + \alpha L$, the right hand side of Equation 11 can be decomposed as:

$$X^\top (\hat{I} + \alpha L) X = X^\top M M^\top X \quad (16)$$

where M can be constructed through Cholesky decomposition. Thus, the generalized eigenvalue problem in Equation 11 can be reformulated as:

$$\frac{1}{\lambda} e = S_1^{-1} U_1^\top X^\top M M^\top X U_1 S_1^{-1} e \quad (17)$$

where $e = S_1 U_1^T \beta$.

Next, if we let $A = S_1^{-1} U_1^T X^T M$, then we can see that this is a traditional eigenvalue problem. A is an $r \times n$ matrix, r is small enough and thus we can decompose it through original SVD naturally: $A = U_2 S_2 V_2^T$. Finally, the embedding matrix can be computed as:

$$B = (U_1 S_1^{-1} e_1, \dots, U_1 S_1^{-1} e_r) = U_1 S_1^{-1} U_2 \quad (18)$$

The original time complexity of the construction of $X^T \Omega \in \mathbb{R}^{d \times n}$ and $X^T M \in \mathbb{R}^{d \times n}$ is $O(d^2 n n_h)$ and $O(d^2 n k)$ respectively, including the computation of the exact k NN for each point, where n_h is the number of samples in each slice. In addition, the time complexity of decomposition of $X^T \Omega$ is $O(n^2 d)$ and the time complexity of construction and computation of Equation 17 is $O(ndr)$. Therefore, the overall time complexity is $O(d^2 n \max(n_h, k) + n^2 d + ndr)$, which is prohibitive in the high-dimensional case.

To alleviate the expensive overhead in high-dimensional case, we use the fast k NN (Achlioptas, 2003; Ailon and Chazelle, 2009) to compute the neighbor information, we find that constructing $X^T \Omega$ and $X^T M$ only requires $O(t d n n_h)$ and $O(t d n k)$ respectively. Moreover, using R-SVD to factorize the matrix $X^T \Omega$ only requires $O(ndr)$. Therefore, The overall time complexity reduces to $O(t d n \max(n_h, k) + ndr)$. t denotes a fixed parameter about the logarithm of n .

Algorithm 2 summarizes the above steps.

Algorithm 2: Randomized semi-supervised dimension reduction

Input: $X_l \in \mathbb{R}^{n_l \times d}$, $X_u \in \mathbb{R}^{n_u \times d}$, number of slice H ; number of nearest neighbor k , effective dimension r

Output: $B \in \mathbb{R}^{d \times r}$

- 1 compute $X^T \Omega$, $X^T M$ from Equation 13 and Equation 16;
 - 2 estimate $[U_1, S_1, V_1] = \text{Randomized SVD}(X^T \Omega, r)$;
 - 3 $A = S_1^{-1} U_1 X^T M$;
 - 4 factorize $[U_2, S_2, V_2] = \text{SVD}(A)$;
 - 5 compute B from Equation 18
-

4.3 Mapping From Low to High

After semi-supervised dimensional reduction, we perform Bayesian optimization with GP on the low-dimensional space \mathcal{Z} . But we need to further consider three issues. The first is how to select the search domain S in the low-dimensional embedding space. The second is how to specify a mapping h associate with B to map the point \mathbf{z} from the embedding space \mathcal{Z} to the high-dimensional space \mathcal{D} where the response value y should be evaluated. The third is how to maintain consistency of the Gaussian process regression model after updating B . Only by addressing these issues, the low-dimensional Bayesian optimization can be updated by the data pair (\mathbf{z}, y) .

Before elaborating the selection of S in the first issue, we introduce the definition of zonotope, which is a convex symmetric polytope.

Definition 1 *Zonotope* (Le et al., 2013) Given a linear mapping $H \in \mathbb{R}^{r \times d}$ and vector $\mathbf{p} \in \mathbb{R}^r$, an r -zonotope is defined as

$$Z = \{\mathbf{z} \in \mathbb{R}^r : \mathbf{z} = \mathbf{p} + H\mathbf{x}; \mathbf{x} \in [-1, 1]^d\}$$

where \mathbf{p} is the center vector of the zonotope.

Without loss of generality, let $\mathbf{p} = \mathbf{0}$, we note that H is exactly B computed by Equation 18. Thus, the zonotope Z_B associate with B is the low-dimensional space where Bayesian optimization is performed. Then, we introduce the smallest box containing the zonotope.

Lemma 2 Given zonotope $Z = \{\mathbf{z} \in \mathbb{R}^r : \mathbf{z} = \mathbf{p} + H\mathbf{x}; \mathbf{x} \in [-1, 1]^d\}$, $\mathbf{p} = \mathbf{0}$, the smallest box containing this zonotope can be computed as

$$S = \left[-\sum_{j=1}^d |H_{1j}|, \sum_{j=1}^d |H_{1j}| \right] \times \cdots \times \left[-\sum_{j=1}^d |H_{rj}|, \sum_{j=1}^d |H_{rj}| \right]$$

Although the boundary of zonotope is difficult to solve, we use the box S as an alternative (Binois et al., 2019).

Next, we focus on the second and third issues. As mentioned before, a mapping h should connect the high-dimensional space and the low-dimensional space. As a result, for any point in the low-dimensional space, a corresponding point can be found in the high-dimensional space. In this way, the low-dimensional point \mathbf{z} and the response value y of the corresponding high-dimensional point \mathbf{x} can be used as the training set to build a Gaussian process regression model. Figure 1 shows the relationship between them. We note that the reproduction of the correlation between \mathbf{z} and y is the goal of the low-dimensional Gaussian process regression model, and the two are closely connected through \mathbf{x} . Thus a reasonable choice of h plays a great influence on such a middle layer. Meanwhile, due to the iterative nature of SILBO, the mapping h will change after updating B , which directly makes the correlation between \mathbf{z} and y inconsistent before and after the update. Therefore, we need to develop a strategy to maintain consistency. Next, we introduce two different strategies to address these two issues.

As shown in Algorithm 3, we can naturally get the response value y by evaluating the point $\mathbf{x} = B^\dagger \mathbf{z}$ after finding the candidate point $\mathbf{z} \in S$ through BO. When the projection matrix B changed, we fix \mathbf{z} at the bottom of the hierarchy in Figure 1a and then update y at the top to maintain consistency (*bottom-up* for short).

Algorithm 3: The *bottom-up* strategy

Input: Labeled low-dimensional points Z_l^t , unlabeled low-dimensional points Z_u^t

Output: Labeled high-dimensional points X_l^t , unlabeled high-dimensional points X_u^t , the training set D_t

- 1 $X_l^t = B_t^\dagger Z_l^t$;
 - 2 $X_u^t = B_t^\dagger Z_u^t$;
 - 3 $Y_t = f(X_l^t)$, $D_t = (Z_l^t, Y_t)$;
-

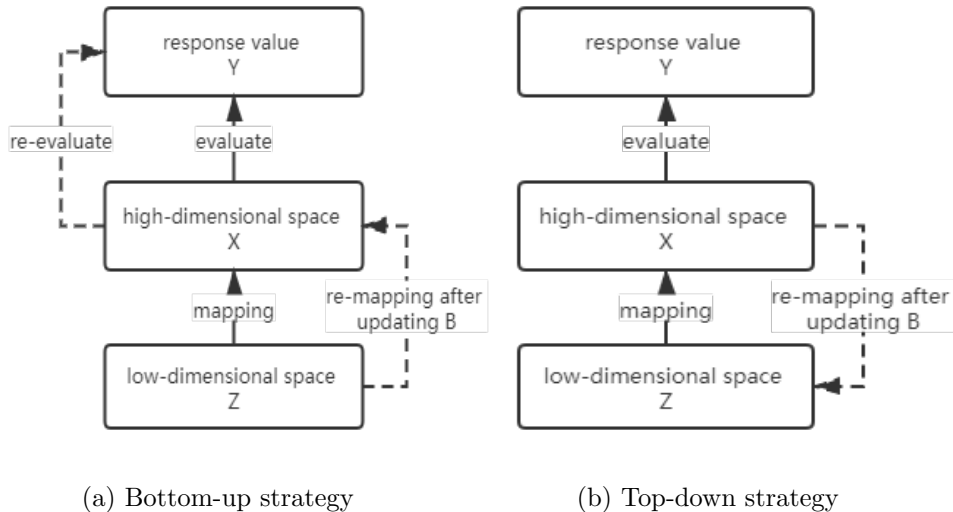


Figure 1: The relationship between response value y , high-dimensional point x , and low-dimensional point z . The solid line shows the process of mapping and evaluation with different strategies. The left hierarchy denotes the *bottom-up* strategy. The dash line shows the process of re-mapping and re-evaluation. z at the bottom is fixed after updating B . Then, re-map z to find and re-evaluate the corresponding x . The right hierarchy shows the *top-down* strategy. The dash line shows the re-mapping process. x and y at the top are fixed after updating B . Then, x is re-mapped to find the corresponding z and a new Gaussian Process regression model will be constructed.

Since we use B^\dagger to connect the points between the low-dimensional space \mathcal{Z} and the high-dimensional space \mathcal{D} , the actual evaluation space ϕ is only a part of \mathcal{D} (i.e., $\phi \subset \mathcal{D}$) when B is fixed. While a great probability of containing the optimum in ϕ has been proved (Wang et al., 2013), one of the preconditions is that there is no limitation to the high-dimensional space of the objective function. In practice, the restriction often exists (e.g., $[-1, 1]^d$), making the high probability no longer guaranteed. In contrast, due to the iterative nature of the effective low-dimensional space learning mechanism in SILBO (Algorithm 1), we can alleviate this problem. Specifically, more and more ϕ associate with B will be learned, which gradually reveal the location of the optimum.

However, the *bottom-up* strategy may bring more evaluation overhead. When we get the training set $D_t = \{z_i, y_i\}_{i=1}^T$ for BO through T iterations in Algorithm 1, we update B to B_{new} and get z_{T+1} through the acquisition function α . Due to the updating of B , the mapping relationship between the high-dimensional and low-dimensional spaces has changed. As shown in Figure 1a, we need to find the corresponding x again for z in the training set and then evaluate x to maintain consistency. When the evaluation of the objective function is expensive, the computational cost is huge.

To eliminate the re-evaluation overhead, we propose a new strategy. Specifically, we first obtain z in the low-dimensional space through the acquisition function α , and then

solve the following equation to find the corresponding \mathbf{x} .

$$\arg \min_{\mathbf{x}} \|\mathbf{B}\mathbf{x} - \mathbf{z}\|^2 \quad (19)$$

When the projection matrix B changed, we fix \mathbf{x} and y at the top of the hierarchy in Figure 1 and then update \mathbf{z} in the bottom to maintain consistency (*top-down* for short).

Algorithm 4: The *top-down* strategy

Input: Labeled low-dimensional points Z_l^t , unlabeled low-dimensional points Z_u^t ,
labeled high-dimensional points X_l^{t-1} , the training set D_{t-1}

Output: labeled high-dimensional points X_l^t , unlabeled high-dimensional points X_u^t ,
the training set D_t

- 1 Get the last point z_l from Z_l^t ;
 - 2 Compute x_l, X_u^t from Equation 19 using z_l, Z_u^t ;
 - 3 $X_l^t = X_l^{t-1} \cup x_l$;
 - 4 $y = f(x_l)$, $D_t = D_{t-1} \cup (z_l, y)$;
-

Different from the *bottom-up* strategy, the *top-down* strategy shown in Figure 1b updates \mathbf{z} directly, which enables us to reconstruct a new BO model efficiently only by replacing the training set with $\{B_{new}\mathbf{x}_i, y_i\}_{i=1}^T$ after updating B , instead of relocating \mathbf{x} and re-evaluating them. The *top-down* strategy can be found in Algorithm 4. Next, we analyze the rationality of this strategy theoretically.

Theorem 3 *Given a matrix $B \in \mathbb{R}^{r \times d}$ with orthogonal rows and its corresponding zonotope Z_B . Given $\mathbf{z} \in Z_B$, for any $\mathbf{x}_1, \mathbf{x}_2 \in U_B = \{\mathbf{x} | \mathbf{x} = B^\top \mathbf{z} + y, \mathbf{x} \in \mathbb{R}^d, y \in N(B)\}$, $B\mathbf{x}_1 = B\mathbf{x}_2 = \mathbf{z}$.*

Proof Let $\mathbf{x} = \mathbf{x}_V + \mathbf{x}_V^\perp \in \mathbb{R}^d$ be the orthogonal decomposition with respect to $V = \text{Row}(B)$, then $\mathbf{x}_V \in V$. Let $\mathbf{z} \in Z_B$ with $B^\top \mathbf{z} = \mathbf{x}_V$. Due to the orthogonal decomposition, we have $\mathbf{x} - \mathbf{x}_V = \mathbf{x} - B^\top \mathbf{z}$ lies in $V^\perp = N(B)$. For any $\mathbf{x}_1, \mathbf{x}_2 \in U_B$, we have $\mathbf{x}_1 - \mathbf{x}_V = \mathbf{x}_1 - B^\top \mathbf{z}$ and $\mathbf{x}_2 - \mathbf{x}_V = \mathbf{x}_2 - B^\top \mathbf{z}$, then $B(\mathbf{x}_1 - B^\top \mathbf{z}) = B(\mathbf{x}_2 - B^\top \mathbf{z}) = 0$. Thus, $B\mathbf{x}_1 = B\mathbf{x}_2 = BB^\top \mathbf{z} = \mathbf{z}$. \blacksquare

According to Theorem 3, if we assume that B has orthogonal rows, it is clear that given B and \mathbf{z} , any point $\mathbf{x} \in U_B$ will be the solution to Equation 19. However, our purpose is not \mathbf{x} itself, but $y = f(\mathbf{x})$, because (\mathbf{z}, y) is the data pair used to update BO. Fortunately, if we use SILBO to learn an ideal effective low-dimensional subspace B^* , then for any $\mathbf{x}_1, \mathbf{x}_2$ in the solution set U_{B^*} , $f(\mathbf{x}_1) = f(B^{*\top} \mathbf{z} + y_1) = f(B^{*\top} \mathbf{z})$, $f(\mathbf{x}_2) = f(B^{*\top} \mathbf{z} + y_2) = f(B^{*\top} \mathbf{z})$ (i.e., $f(\mathbf{x}_1) = f(\mathbf{x}_2)$). Thus, in each iteration T , we can obtain the unique data pair (\mathbf{z}_T, y_T) under B^* to update the low-dimensional Bayesian optimization model. Therefore, the diversity of solutions in the set U_B does not affect the construction of BO and we can explore in the original space \mathcal{D} which liberates the shackles of ϕ .

In summary, both the two strategies aim to generate a consistent training set for the subsequent GP construction when updating B . To maintain such consistency, the *bottom-up* strategy acquires more observations y from the objective function according to \mathbf{z} in the

training set while the *top-down* strategy directly changes \mathbf{z} according to y . Note that the more response values, the more information about the objective function we can get. Thus, the *bottom-up* strategy can obtain more clues about the global optimum than the *top-down* strategy.

5. Numerical Results

In this section, we evaluated our proposed algorithm SILBO on a set of high-dimensional benchmarks. First, we compared SILBO with other state-of-the-art algorithms on synthetic function² and neural network hyperparameter optimization tasks. Second, we evaluated and analyzed the scalability of SILBO. Finally, we demonstrated the effectiveness of semi-supervised embedding learning.

5.1 Experiment Setting

For comparison, we also evaluated with other state-of-the-art algorithms: REMBO (Wang et al., 2013), which performs BO on random linear embedding, REMBO- K_X (Nayebi et al., 2019) which computes the kernel using distance in the high-dimensional space. REMBO- K_ψ (Binois et al., 2015), which uses a warping kernel and finds the evaluation point through sophisticated mapping. HeSBO (Nayebi et al., 2019), which uses the count-sketch technique to generate subspace and compute the projection matrix. Additional baselines include ADD-BO (Kandasamy et al., 2015), which assumes that the objective function has an additive structure, and recently-proposed SIR-BO (Zhang et al., 2019), which uses SIR to learn a low-dimensional space actively. SILBO-BU and SILBO-TD represent the proposed SILBO algorithm that employs the *bottom-up* and *top-down* mapping strategies respectively.

We employed the package *GPy*³ as the Gaussian Process framework and selected the Matrn kernel for the GP model. We adopted the package *ristretto*⁴ to perform the R-SVD. The embedding matrix B was set to be updated every 20 iterations. We employed *CMA-ES* (Hansen, 2016) to compute Equation 19 for SILBO-TD. The size of the unlabeled points is set to 50 in each iteration. The number of neighbors k is set to 7 for semi-supervised dimension reduction. To obtain error bars, we performed 100 independent runs for each algorithm on synthetic functions and 5 runs for the neural network hyperparameter search. We plotted the mean value along with one standard deviation. For ADD-BO, we used the authors' implementation through *MATLAB*, so we did not compare its scalability since other algorithms were implemented in *Python*. Also, we evaluated SILBO using two acquisition functions: UCB and EI.

5.2 Performance on Synthetic Functions

Similar to (Nayebi et al., 2019), these algorithms were under comparison upon the following widely-used test functions: (1) Branin (2) Colville (3) Hartmann-6. The active dimensionalities for Branin, Colville, Hartmann-6 are 2, 4, and 6 respectively. We studied the cases with different input dimensions $d \in \{100, 1000\}$. The experimental results are shown

2. The synthetic function can be found at <https://www.sfu.ca/~ssurjano/optimization.html>.

3. <https://github.com/SheffieldML/GPy>

4. <https://github.com/erichson/ristretto>

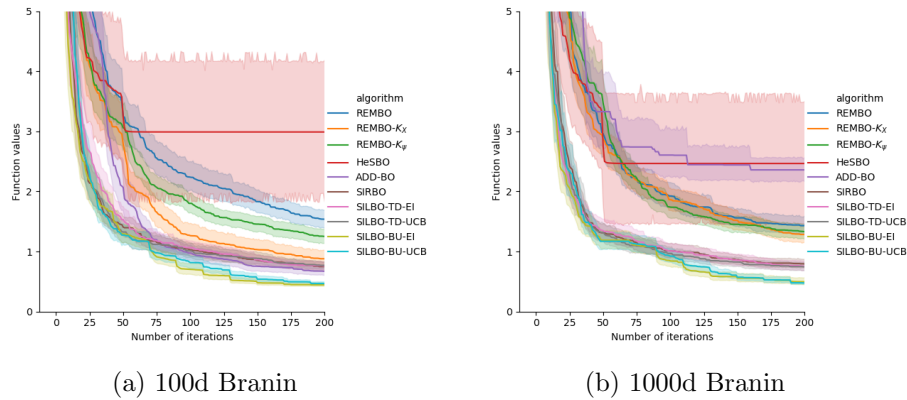


Figure 2: Performance on Branin under dimension 100(a) and dimension 1000(b) with embedding dimension $r = 2$. We plotted mean and one standard deviation across 100 independent runs.

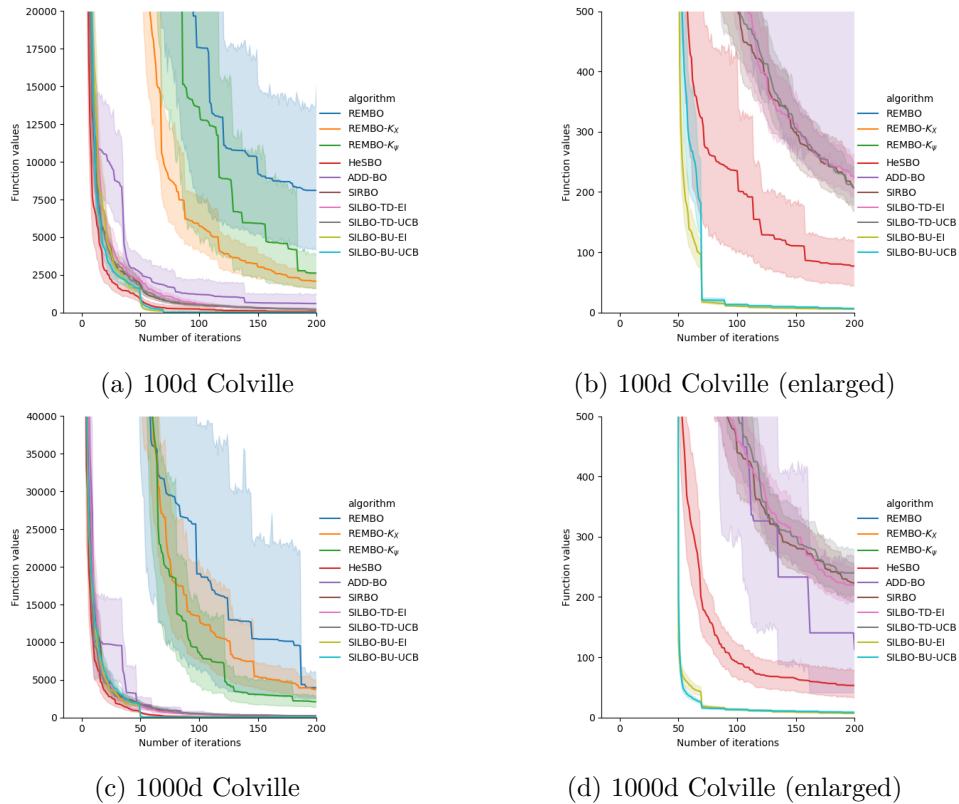


Figure 3: Performance on Colville under dimension 100(a)(b) and dimension 1000(c)(d) with embedding dimension $r = 4$. To see performance discrepancy clearly among different algorithms, we enlarged (a)(c) to get (b)(d) respectively. We plotted mean and one standard deviation across 100 independent runs.

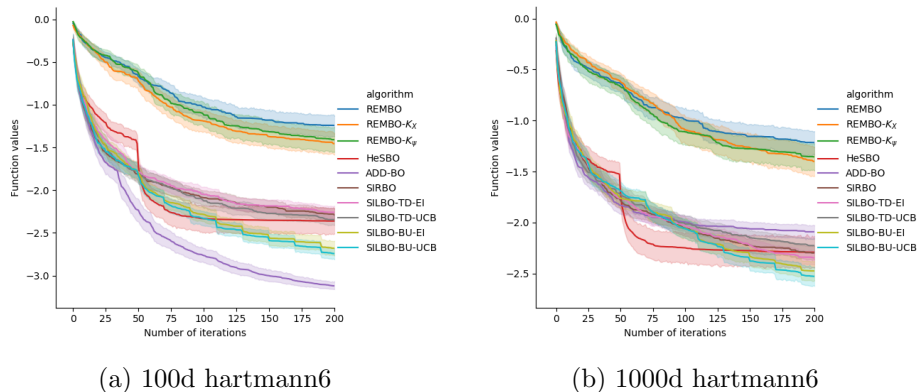


Figure 4: Performance on Hartmann6 under dimension 100(a) and dimension 1000(b) with embedding dimension $r = 6$. We plotted mean and one standard deviation across 100 independent runs.

in Figure 2-4. The proposed SILBO-BU, outperforms all benchmarks especially in high dimensions ($d = 1000$). SILBO-TD is also very competitive, surpassing most traditional algorithms. In addition, the experimental results under different acquisition functions are similar. ADD-BO performs excellently in Hartmann-6 due to the additive structure of the function itself. However, it performs poorly in higher dimensions and functions without the additive assumption. HeSBO performs well in Colville and Hartmann-6, but poorly in Branin. Moreover, we can find that HeSBO does not converge in most cases. The performance of SIRBO is similar to our proposed SILBO-TD since it also tries to learn an embedding space actively. In contrast, the proposed method SILBO-BU nearly beats all baselines due to its powerful iterative embedding learning.

5.3 Hyperparameter Optimization on Neural Network

Following (Oh et al., 2018), we also evaluated SILBO in the hyperparameter optimization task for a neural network on the *MNIST* dataset. Specifically, the neural network has one hidden layer of size 50 and one output layer of size 10. These 500 initial weights are viewed as hyperparameters and optimized using Adam (Kingma and Ba, 2015).

Figure 5 shows that SILBO-BU converges quickly than all other benchmarks. The performance of HeSBO also improves quickly but converged slowly to the optimum. The performance of SILBO-TD and SIRBO is close. The two methods perform better than other traditional benchmarks such as REMBO and show competitive performance. Specifically, we can see that the curve corresponding to SILBO-BU obtained a better response value every 20 iterations, which demonstrate the effectiveness of our iterative embedding learning.

5.4 Scalability Analysis

We analyzed the scalability by comparing the cumulative time of each algorithm under the same number of iterations. As shown in Figure 6, we can see that for the low-cost objective functions such as Branin, SILBO-BU is fast, while SILBO-TD is relatively slow. This is because CMA-ES is used to solve Equation 19, which takes much time. For the expensive

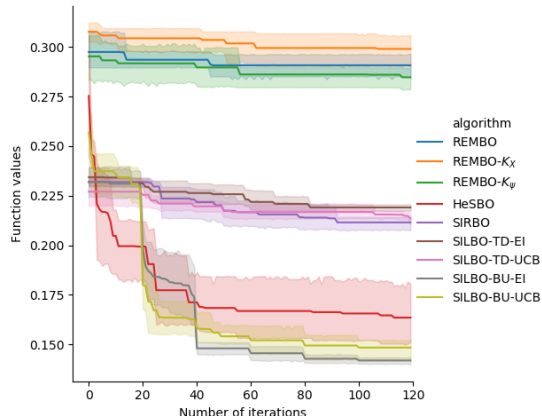
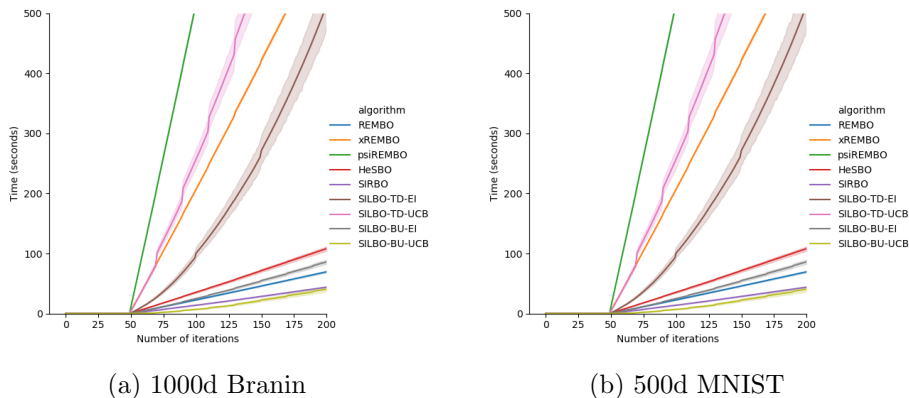


Figure 5: Performances on the neural network with embedding dimension $r=12$. We plotted mean and one standard deviation across 5 independent runs.



(a) 1000d Branin

(b) 500d MNIST

Figure 6: Comparison of the cumulative time on Branin(a) with dimension 1000 and on neural network(b) with dimension 500.

objective functions such as neural networks, SILBO-TD takes approximately the same time as most algorithms, while SILBO-BU takes more time due to its re-evaluation process.

5.5 Effectiveness of Embedding Learning

We compared the embedding learning performance of SILBO and SIR on Branin and Camel. We first evaluated 50 high-dimensional points to get response value and then projected these points to low-dimensional space. The goal is to find the e.d.r directions that preserve the information of the objective function as comprehensively as possible. Figure 7 and Figure 8 summarize the observed performance.

We can see that the information extracted by the SIR method stacked together. A specific low-dimensional point corresponds to many different response values. The consequence is that a lot of information will be lost if we train a Gaussian process regression model using

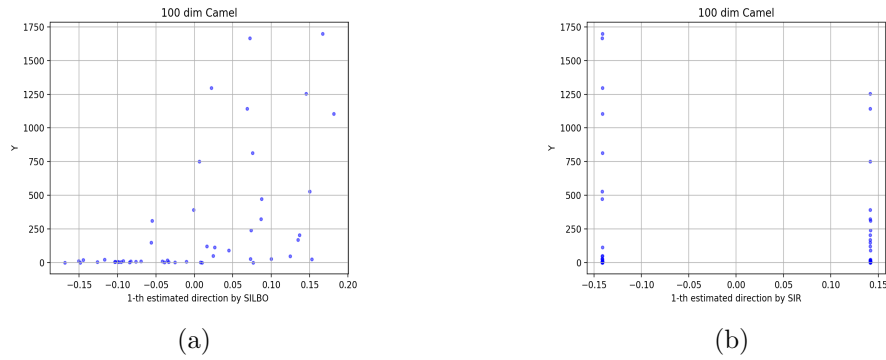


Figure 7: (a) and (b) show the information extracted by SILBO and SIR respectively on Camel. The number of e.d.r directions is set to 1.

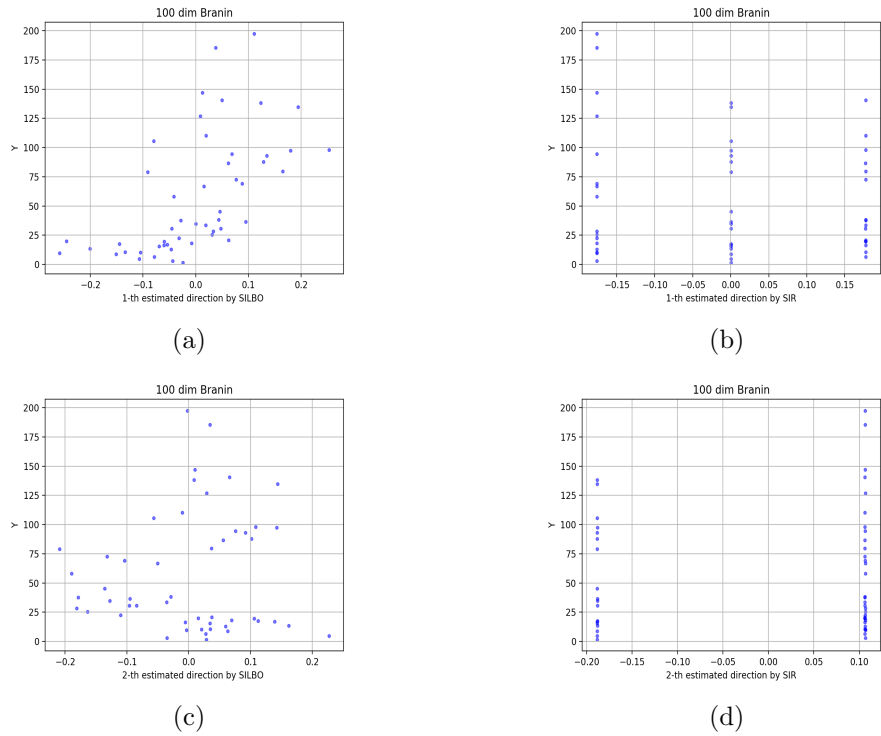


Figure 8: (a)(c) and (b)(d) show the information extracted by SILBO and SIR respectively on Branin. The number of e.d.r directions is set to 2. (a)(b) plot the points projected to one estimated direction and their corresponding response values. (c)(d) plot the points projected to the other direction.

these low-dimensional representations. In contrast, the information extracted by SILBO is complete without the loss of the intrinsic information of the objective function.

6. Conclusion and Future Work

In this paper, we proposed a novel iterative embedding learning framework SILBO for high-dimensional Bayesian optimization through semi-supervised dimensional reduction. We also proposed a randomized fast algorithm for solving the embedding matrix efficiently. Moreover, according to the cost of the objective function, two different mapping strategies are proposed. Experimental results on both synthetic function and hyperparameter optimization tasks reveal that SILBO outperforms the existing state-of-the-art high-dimensional Bayesian optimization methods. In the future, we plan to combine our framework with the multi-fidelity method. Moreover, we also plan to apply SILBO to more AutoML (Automatic Machine Learning) tasks.

Acknowledgments

This work was supported by the National Natural Science Foundation of China (U1811461, 61702254), National Key R&D Program of China (2019YFC1711000), Jiangsu Province Science and Technology Program (BE2017155), National Natural Science Foundation of Jiangsu Province (BK20170651), and Collaborative Innovation Center of Novel Software Technology and Industrialization.

References

- Dimitris Achlioptas. Database-friendly random projections: Johnson-lindenstrauss with binary coins. *Journal of Computer and System Sciences*, 66(4):671 – 687, 2003.
- Nir. Ailon and Bernard. Chazelle. The fast johnsonlindenstrauss transform and approximate nearest neighbors. *SIAM Journal on Computing*, 39(1):302–322, 2009.
- Mikhail Belkin and Partha Niyogi. Laplacian eigenmaps and spectral techniques for embedding and clustering. In *Proceedings of the 14th International Conference on Neural Information Processing Systems: Natural and Synthetic*, NIPS01, page 585591, Cambridge, MA, USA, 2001.
- James Bergstra, Rémi Bardenet, Yoshua Bengio, and Balázs Kégl. Algorithms for hyperparameter optimization. In *Proceedings of the 24th International Conference on Neural Information Processing Systems*, NIPS11, page 25462554, Red Hook, NY, USA, 2011.
- Mickaël Binois, David Ginsbourger, and Olivier Roustant. A warped kernel improving robustness in bayesian optimization via random embeddings. In *Learning and Intelligent Optimization*, pages 281–286, Cham, 2015.
- Mickal Binois, David Ginsbourger, and Olivier Roustant. On the choice of the low-dimensional domain for global optimization via random embeddings. *Journal of Global Optimization*, 2019.
- D. Cai, X. He, and J. Han. Semi-supervised discriminant analysis. In *2007 IEEE 11th International Conference on Computer Vision*, pages 1–7, Oct 2007.
- F. R. K. Chung. *Spectral Graph Theory*. American Mathematical Society, 1997.
- Josip Djolonga, Andreas Krause, and Volkan Cevher. High-dimensional gaussian process bandits. In *Advances in Neural Information Processing Systems 26*, pages 1025–1033, 2013.
- Stephan Eissman, Daniel Levy, Rui Shu, Stefan Bartzsch, and Stefano Ermon. Bayesian optimization and attribute adjustment. In *Proc. 34th Conference on Uncertainty in Artificial Intelligence*, 2018.
- Peter I. Frazier. A Tutorial on Bayesian Optimization. art. arXiv:1807.02811, 2018.
- Jacob Gardner, Chuan Guo, Kilian Weinberger, Roman Garnett, and Roger Grosse. Discovering and Exploiting Additive Structure for Bayesian Optimization. In *Proceedings of the 20th International Conference on Artificial Intelligence and Statistics*, volume 54 of *Proceedings of Machine Learning Research*, pages 1311–1319, Fort Lauderdale, FL, USA, 20–22 Apr 2017.
- Stoyan Georgiev and Sayan Mukherjee. Randomized Dimension Reduction on Massive Data. art. arXiv:1211.1642, 2012.

- Rafael Gmez-Bombarelli, Jennifer N. Wei, David Duvenaud, Jos Miguel Hernandez-Lobato, Benjamn Snchez-Lengeling, Dennis Sheberla, Jorge Aguilera-Iparraguirre, Timothy D. Hirzel, Ryan P. Adams, and Aln Aspuru-Guzik. Automatic chemical design using a data-driven continuous representation of molecules. *ACS Central Science*, 4(2):268–276, 2018.
- N. Halko, P. G. Martinsson, and J. A. Tropp. Finding structure with randomness: Probabilistic algorithms for constructing approximate matrix decompositions. *SIAM Review*, 53(2):217–288, 2011.
- Nikolaus Hansen. The CMA Evolution Strategy: A Tutorial. *arXiv e-prints*, art. arXiv:1604.00772, April 2016.
- Daniel Hernández-Lobato, José Miguel Hernández-Lobato, Amar Shah, and Ryan P. Adams. Predictive entropy search for multi-objective bayesian optimization. In *Proceedings of the 33rd International Conference on International Conference on Machine Learning - Volume 48*, ICML16, page 14921501. JMLR.org, 2016.
- Frank Hutter, Holger H. Hoos, and Kevin Leyton-Brown. Sequential model-based optimization for general algorithm configuration. In *Learning and Intelligent Optimization*, pages 507–523, Berlin, Heidelberg, 2011.
- Kirthevasan Kandasamy, Jeff Schneider, and Barnabás Póczos. High dimensional bayesian optimisation and bandits via additive models. In *Proceedings of the 32nd International Conference on International Conference on Machine Learning - Volume 37*, ICML15, page 295304, 2015.
- Kirthevasan Kandasamy, Gautam Dasarathy, Jeff Schneider, and Barnabás Póczos. Multifidelity bayesian optimisation with continuous approximations. In *Proceedings of the 34th International Conference on Machine Learning - Volume 70*, ICML17, page 17991808, 2017.
- Kirthevasan Kandasamy, Willie Neiswanger, Jeff Schneider, Barnabás Póczos, and Eric P. Xing. Neural architecture search with bayesian optimisation and optimal transport. In *Proceedings of the 32nd International Conference on Neural Information Processing Systems*, NIPS18, page 20202029, Red Hook, NY, USA, 2018.
- Diederik P. Kingma and Jimmy Ba. Adam: A method for stochastic optimization. In *3rd International Conference on Learning Representations, ICLR 2015, San Diego, CA, USA, May 7-9, 2015, Conference Track Proceedings*, 2015.
- Aaron Klein, Stefan Falkner, Simon Bartels, Philipp Hennig, and Frank Hutter. Fast Bayesian Optimization of Machine Learning Hyperparameters on Large Datasets. In Aarti Singh and Jerry Zhu, editors, *Proceedings of the 20th International Conference on Artificial Intelligence and Statistics*, volume 54 of *Proceedings of Machine Learning Research*, pages 528–536, Fort Lauderdale, FL, USA, 20–22 Apr 2017. PMLR.
- Vu Tuan Hieu Le, Cristina Stoica, T. Alamo, E.F. Camacho, and Didier Dumur. *Zonotopes: From Guaranteed State Estimation to Control*. Wiley-ISTE, October 2013.

- Ker-Chau Li. Sliced inverse regression for dimension reduction. *Journal of the American Statistical Association*, 86(414):316–327, 1991.
- Xiaoyu Lu, Javier Gonzalez, Zhenwen Dai, and Neil Lawrence. Structured variationally auto-encoded optimization. In *Proceedings of the 35th International Conference on Machine Learning*, volume 80 of *Proceedings of Machine Learning Research*, pages 3267–3275, Stockholmsmssan, Stockholm Sweden, 10–15 Jul 2018.
- Riccardo Moriconi, Marc P. Deisenroth, and K. S. Sesh Kumar. High-dimensional Bayesian optimization using low-dimensional feature spaces. *arXiv e-prints*, art. arXiv:1902.10675, February 2019.
- Amin Nayebi, Alexander Munteanu, and Matthias Poloczek. A framework for Bayesian optimization in embedded subspaces. In Kamalika Chaudhuri and Ruslan Salakhutdinov, editors, *Proceedings of the 36th International Conference on Machine Learning*, volume 97 of *Proceedings of Machine Learning Research*, pages 4752–4761, Long Beach, California, USA, 09–15 Jun 2019.
- ChangYong Oh, Efstratios Gavves, and Max Welling. Bock : Bayesian optimization with cylindrical kernels. *ICML*, pages 3865–3874, 2018.
- B. Shahriari, K. Swersky, Z. Wang, R. P. Adams, and N. de Freitas. Taking the human out of the loop: A review of bayesian optimization. *Proceedings of the IEEE*, 104(1):148–175, 2016.
- Jasper Snoek, Hugo Larochelle, and Ryan P. Adams. Practical bayesian optimization of machine learning algorithms. In *Proceedings of the 25th International Conference on Neural Information Processing Systems - Volume 2*, NIPS12, page 29512959, Red Hook, NY, USA, 2012.
- Niranjan Srinivas, Andreas Krause, Sham Kakade, and Matthias Seeger. Gaussian process optimization in the bandit setting: No regret and experimental design. In *Proceedings of the 27th International Conference on International Conference on Machine Learning*, ICML10, page 10151022, Madison, WI, USA, 2010.
- Kevin Swersky, Jasper Snoek, and Ryan P. Adams. Multi-task bayesian optimization. In *Proceedings of the 26th International Conference on Neural Information Processing Systems - Volume 2*, NIPS13, page 20042012, Red Hook, NY, USA, 2013.
- Ziyu Wang, Masrour Zoghi, Frank Hutter, David Matheson, and Nando De Freitas. Bayesian optimization in high dimensions via random embeddings. In *Proceedings of the Twenty-Third International Joint Conference on Artificial Intelligence*, IJCAI 13, page 17781784, 2013.
- Jian Wu, Matthias Poloczek, Andrew Gordon Wilson, and Peter I. Frazier. Bayesian optimization with gradients. In *Proceedings of the 31st International Conference on Neural Information Processing Systems*, NIPS17, page 52735284, Red Hook, NY, USA, 2017.
- Jian Wu, Saul Toscano-Palmerin, I. Peter Frazier, and Gordon Andrew Wilson. Practical multi-fidelity bayesian optimization for hyperparameter tuning. *UAI*, 2019.

Qiang Wu, Feng Liang, and Sayan Mukherjee. Localized sliced inverse regression. *Journal of Computational and Graphical Statistics*, 19(4):843–860, 2010.

Miao Zhang, Huiqi Li, and Steven Su. High dimensional bayesian optimization via supervised dimension reduction. In *Proceedings of the Twenty-Eighth International Joint Conference on Artificial Intelligence, IJCAI-19*, pages 4292–4298, 7 2019.